

Expanding the Repertoire of Chalcogenide Nanocrystal Networks: Ag₂Se Gels and Aerogels by Cation Exchange Reactions

Qinghong Yao, Indika U. Arachchige, and Stephanie L. Brock*

Department of Chemistry, Wayne State University, Detroit, Michigan 48202

Received January 4, 2009; E-mail: sbrock@chem.wayne.edu

An aerogel is a unique class of material consisting of a highly porous network composed of connected nanoscale building blocks. The presence of an interconnected network of pores, including both micropores (<2 nm) and mesopores (2–50 nm), with a high inner surface area nanostructure is expected to lead to many actual and potential applications in catalysis, solar cells, and sensors.^{1,2} However, conventional aerogels are based on oxides and traditionally focused on insulating or wide band gap materials, such as SiO₂, TiO₂, and Al₂O₃.³ Recently, the aerogel family has been extended to semiconducting metal chalcogenide aerogels (PbS, CdSe, CdS, ZnS), enabling band gap tuning through the visible region.⁴ The aerogels are prepared by partial oxidative removal of thiolate capping groups from the corresponding metal chalcogenide nanoparticle surface to form a wet gel, followed by supercritical solvent extraction. The obtained aerogels retain the inherent nanoparticle properties: specifically, quantum confinement effects, average pore sizes in the mesoporous regime, and very high surface areas. Among these aerogels, the synthesis of CdSe aerogels is the best developed and has been optimized to yield robust monoliths.⁵

Although the sol–gel assembly of nanoparticles has been shown to be a powerful tool for the preparation of metal chalcogenide aerogels, the chemistry is limited to nanoparticles with established syntheses and to compositions that are robust to gelation conditions. To expand the repertoire of chemistries that can be accessed within the aerogel framework, alternative synthetic methods are desired. Cation exchange reactions have been demonstrated as useful and simple methods for preparing new compositions of thin films and nanoparticles without having to build the new films or nanoparticles from the bottom-up. For example, the transformation of binary metal chalcogenide nanocrystals, CdQ → M_xQ_y (Q = S, Se, Te; M = Ag, Pb, Pt, Pd, Cu), has been demonstrated by treatment of CdQ with appropriate ions.^{6,7} While these reactions may be thermodynamically favored by a large difference in solubility (e.g., $K_{sp} = 1.0 \times 10^{-33}$ and 3.1×10^{-65} for CdSe and Ag₂Se, respectively),^{8,9} the conversion reaction is kinetically prohibited at ambient conditions in the bulk because of the high activation energy required for the diffusion of ions in the solid lattice framework.⁷ However, the activation barrier decreases as particle size decreases, enabling exchange to occur within seconds for nanoparticles.⁶ Importantly, this approach is not limited to discrete nanoparticles; liquid crystal templated mesostructures can also be transformed and without losing their mesoscale order.¹⁰

Because metal chalcogenide gels are formed from nanoscale building blocks, we surmised that a kinetically rapid mechanism of cation exchange would take place in the gel system as well. This would enable efficient production of new aerogel compositions without the need to synthesize each individual nanoparticle phase or figure out the vagaries of synthesis and ligand modification of different building blocks as well as optimal gelation conditions for rendering monoliths with minimal surface oxidation. In the present study, we show that Ag₂Se wet gel monoliths can be prepared by

an ion-exchange reaction of a monolithic CdSe wet gel and converted to an aerogel by drying under supercritical conditions. Importantly, the conversion is essentially topotactic, suggesting the transformation is achieved without greatly affecting the morphology or particle interconnectivity. This demonstrates both the integrity and accessibility of the chalcogenide gel networks.

CdSe nanoparticles, thiolate-exchanged nanoparticles, and wet gels resulting from oxidative decomplexation were synthesized according to literature methods⁵ (Supporting Information, SI). To conduct the ion exchange, 4 mL of a 0.15 M AgNO₃ methanol solution were added to one monolithic CdSe wet gel immersed in methanol (assembled from 4 mL of CdSe sol ([Cd²⁺] = 0.025 M)) without disturbance of the gel framework. The orange color of the CdSe gel turned black immediately. After 12 h, the exchanged wet gel was solvent exchanged with 4 mL of methanol 4–5 times per day for two days to remove excess Ag⁺ ions and exchanged Cd²⁺ ions. The resultant wet gel was solvent exchanged with acetone prior to supercritical CO₂ drying. As shown in Figure 1A, the monolithic wet gel framework (left) was retained all through the exchange (middle) and drying (right) processes, suggesting the dominant process in the exchange is limited to diffusion of cations through the anion sublattice of the individual nanoparticle building blocks. The subsequent supercritical drying process allows solvent (liquid CO₂) to be removed from the pores without collapse, thereby producing a dry gel of similar volume and monolithic shape to the wet gel (i.e., an aerogel).

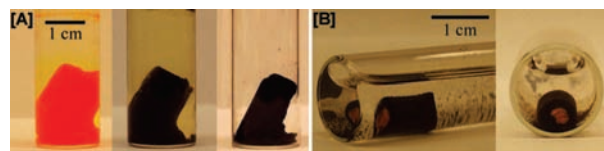


Figure 1. [A] Photograph of initial CdSe wet gel (left), Ag⁺ exchanged CdSe wet gel (middle), and resultant Ag₂Se aerogel (right); [B] photograph of partially exchanged CdSe wet gel, sliced in two.

The completion of the ion-exchange process is confirmed by energy dispersive spectroscopy (EDS), UV/vis/NIR absorption (converted from reflectance), and photoluminescence spectra (SI). EDS spectra of aerogels produced from supercritical drying of Ag⁺ exchanged CdSe wet gels exhibit three dominant peaks corresponding to Ag, Se, and S. No Cd peak is observed. The atomic ratio of Ag/Se is 2:1, consistent with the formulation Ag₂Se. A small amount of S (9%) is present, which we attribute to residual (i.e., unreacted) thiolate surface groups present in the gel. The exchanged aerogel shows no absorption or emission of light in the range 500 to 800 nm, where the corresponding CdSe aerogels are optically active.

The phase and crystallinity of the exchanged product were analyzed by powder X-ray diffraction (PXRD). When compared to the corresponding CdSe aerogel (Figure 2A), the synthesized Ag₂Se aerogel adopts a body-centered cubic phase (α -phase) with

Ag^+ distributed over tetrahedral interstitial sites (Figure 2B), distinct from the hexagonal CdSe precursor. The crystallite size of the Ag_2Se aerogel is calculated to be 3.6 nm (peak at 44°) by using a modified Scherrer formula, suggesting only modest crystallite growth has occurred relative to the corresponding CdSe aerogel, 2.8 nm (peak at 35°).

The formation of $\alpha\text{-Ag}_2\text{Se}$ is notable because orthorhombic $\beta\text{-Ag}_2\text{Se}$ is the thermodynamically stable form at room temperature. The intrinsic disordered cation lattice in $\alpha\text{-Ag}_2\text{Se}$ is associated with superionic conductivity,¹¹ which has precipitated efforts to stabilize this form at room temperature for potential battery applications. This intrinsic structural disorder may explain the breadth of the peak at 36° for the Ag_2Se aerogel, which is consistent with an amorphous component (SI), and is also seen for Ag_2Se nanoparticles made from ion exchange of CdSe nanoparticles.⁶

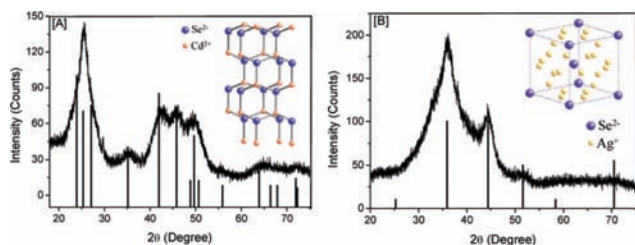


Figure 2. PXRD pattern of the CdSe aerogel [A] and corresponding Ag_2Se aerogel [B]. The ICDD-PDF overlays of hexagonal CdSe (PDF # 08-0459) and cubic Ag_2Se (PDF # 27-0619) are shown as lines in [A] and [B], respectively. The inset images show the crystal structure of hexagonal CdSe [A] and cubic Ag_2Se (cation sites partially occupied) [B].

The morphology of the aerogels was studied by transmission electron microscopy (TEM) (Figure 3 and SI). The typical pearl-necklace morphology of colloidal aerogels is observed in both cases, with the primary nanoscale particles clearly evident, and both aerogels exhibit a broad range of pores extending from the meso- (2–50 nm) into the macro- (>50 nm) porous regime.

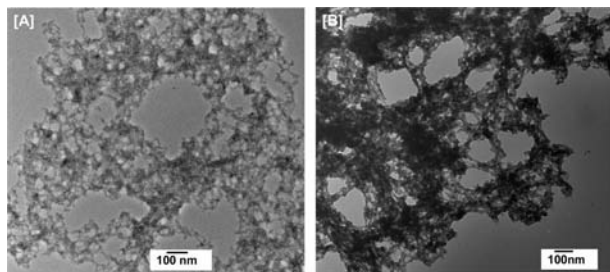


Figure 3. TEM image of CdSe [A] and Ag_2Se [B] aerogels.

The surface area and pore size distribution for Ag_2Se aerogels were determined by N_2 adsorption/desorption isotherms (SI) and are consistent with electron micrograph images. The isotherms are similar to those previously observed for CdSe aerogels⁵ as is the pore-size distribution (BJH) plot, which suggests a characteristically broad range of pores (2–120 nm), with a somewhat higher average pore diameter (Table 1). The relatively lower surface area for Ag_2Se compared to CdSe actually translates to a higher per mole surface area. This is shown when the equivalent surface area of silica (a “standard” aerogel phase) is computed for Ag_2Se and CdSe by considering the relative formula masses (Table 1 and SI).

Table 1. Porosimetry Data for CdSe and Ag_2Se Aerogels

sample	BET surface area (m^2/g)	silica equivalence BET surface area (m^2/g) ^a	BJH average pore diameter (nm)	BJH cumulative pore volume (cm^3/g)
CdSe aerogel	133	424	16	0.58
Ag_2Se aerogel	111	548	22	0.69

^a Silica equivalence surface areas were computed by converting the BET surface area for 1 mol of CdSe or Ag_2Se aerogel into that for 1 mol of SiO_2 using respective compound formula masses.

The present study shows that the cation-exchange reaction is a simple and efficient way to prepare Ag_2Se wet gels and aerogels from CdSe gel precursors. The striking similarity in crystallite size, morphology, and surface area characteristics supports a mechanism in which the bonding within the gel network remains globally unchanged, even as the structural attributes of the nanoparticle components are undergoing a dramatic transformation. The obtained fully converted Ag_2Se aerogel has potential applications in batteries and electronic sensors, considering that $\alpha\text{-Ag}_2\text{Se}$ exhibits superionic conductivity,¹¹ and these can be expected to benefit from a nanostructured formulation with a large interfacial surface area. The ion-exchange synthesis route can also be successfully employed for other gel systems, e.g., PbSe and CuSe (SI).

Intuitively, the rapid exchange also enables exquisite control of composition on the macroscale, governed by the diffusion process through the gel network. Instead of exchanging just the surface of individual nanoparticle components, rapid and complete exchange is obtained within the diffusion zone. By control of the amount of exchanging ion added, partial cation exchange can be achieved, as shown in Figure 1B, in which the outer surface of the gel body is transformed into Ag_2Se (black), while the core is still CdSe (orange). This represents a nanostructure with two components of mm–cm dimensions. Thus, the partial ion-exchange mechanism opens the door to making heterogeneous composite aerogels that may be useful for applications requiring hierarchical nanostructured architectures.

Acknowledgment. This work was supported by NSF (DMR-0701161) and ACS-PRF (43550-AC10). We thank Dr. Yi Liu for help with TEM.

Supporting Information Available: Experimental details and data plots for Ag_2Se , PbSe, and CuSe. This material is available free of charge via the Internet at <http://pubs.acs.org>.

References

- Rolison, D. R. *Science* **2003**, *299*, 1698–1701.
- Long, J. W.; Rolison, D. R. *Acc. Chem. Res.* **2007**, *40*, 854–862.
- Hüsing, N.; Schubert, U. *Angew. Chem., Int. Ed.* **1998**, *37*, 22–45.
- Mohanan, J. L.; Arachchige, I. U.; Brock, S. L. *Science* **2005**, *307*, 397–400.
- Arachchige, I. U.; Brock, S. L. *J. Am. Chem. Soc.* **2006**, *128*, 7964–7971.
- Son, D. H.; Hughes, S. M.; Yin, Y.; Alivisatos, A. P. *Science* **2004**, *306*, 1009–1012.
- Wark, S. E.; Hsia, C.; Son, D. H. *J. Am. Chem. Soc.* **2008**, *130*, 9550–9555.
- Woodbury, H. H. *Phys. Rev.* **1964**, *134*, A492.
- Dzhafarov, T. D.; Serin, M.; Ören, D.; Süngü, B.; Sadigov, M. S. *J. Phys. D: Appl. Phys.* **1999**, *32*, L5–L8.
- Lubeck, C. R.; Han, T. Y.; Gash, A. E.; Satcher, J. H., Jr.; Doyle, F. M. *Adv. Mater.* **2006**, *18*, 781–784.
- Boalchand, P.; Bresser, W. J. *Nature* **2001**, *410*, 1070–1073.

JA900042Y